JCI The Journal of Clinical Investigation

# Antigenic sites in influenza H1 hemagglutinin display species-specific immunodominance

Sean T. H. Liu, … , Florian Krammer, Peter Palese

*J Clin Invest.* 2018. https://doi.org/10.1172/JCI122895.

**Concise Communication** **Immunology** **Virology**

Hemagglutination inhibition (HI) titers are a major correlate of protection for influenza-related illness. The influenza virus hemagglutinin possesses antigenic sites that are the targets of HI active antibodies. Here, a panel of mutant viruses each lacking a classically defined antigenic site was created to compare the species-specific immunodominance of the antigenic sites in a clinically relevant hemagglutinin. HI active antibodies of antisera from influenza virus–infected mice targeted sites Sb and Ca2. HI active antibodies of guinea pigs were not directed against any specific antigenic site, although trends were observed toward Sb, Ca2, and Sa. HI titers of antisera from infected ferrets were significantly affected by site Sa. HI active antibodies of adult humans followed yet another immunodominance pattern, in which sites Sb and Sa were immunodominant. When comparing the HI profiles among different species by antigenic cartography, animals and humans grouped separately. This study provides characterizations of the antibody-mediated immune responses against the head domain of a recent H1 hemagglutinin in animals and humans.



# Antigenic sites in influenza H1 hemagglutinin display species-specific immunodominance

Sean T. H. Liu,[1,2] Mohammad Amin Behzadi,[1] Weina Sun,[1] Alec W. Freyn,[1] Wen-Chun Liu,[1] Felix Broecker,[1] Randy A. Albrecht,[1,3] Nicole M. Bouvier,[1,2] Viviana Simon,[1,3] Raffael Nachbagauer,[1] Florian Krammer,[1] and Peter Palese[1]

[1]Department of Microbiology, [2]Division of Infectious Diseases, and [3]Global Health and Emerging Pathogens Institute, Icahn School of Medicine at Mount Sinai, New York, New York, USA.

**Hemagglutination inhibition (HI) titers are a major correlate of protection for influenza-related illness. The influenza virus hemagglutinin possesses antigenic sites that are the targets of HI active antibodies. Here, a panel of mutant viruses each lacking a classically defined antigenic site was created to compare the species-specific immunodominance of the antigenic sites in a clinically relevant hemagglutinin. HI active antibodies of antisera from influenza virus–infected mice targeted sites Sb and Ca2. HI active antibodies of guinea pigs were not directed against any specific antigenic site, although trends were observed toward Sb, Ca2, and Sa. HI titers of antisera from infected ferrets were significantly affected by site Sa. HI active antibodies of adult humans followed yet another immunodominance pattern, in which sites Sb and Sa were immunodominant. When comparing the HI profiles among different species by antigenic cartography, animals and humans grouped separately. This study provides characterizations of the antibody-mediated immune responses against the head domain of a recent H1 hemagglutinin in animals and humans.**

## Introduction

Each year influenza viruses cause significant morbidity and mortality on a global scale (1). Seasonal vaccination is currently the most effective intervention against influenza (2), yet overall vaccine effectiveness was only 36% in the recent 2017–2018 season (3). Development of more effective influenza virus vaccines requires a deeper understanding of the host immune responses (4, 5). The pandemic-like H1N1 influenza virus strain, A/Michigan/45/2015, was recently included as a component of the seasonal influenza vaccine (6) and has been recommended as a vaccine component for the 2018–2019 northern hemisphere influenza season. This study characterizes the antigenicity of 5 classically defined antigenic sites within the hemagglutinin (HA) head domain of this H1 strain in animals and humans.

Influenza virus is an 8-segmented, single-stranded, negative-sense RNA virus of the family *Orthomyxoviridae* (7). The immunodominant surface protein, HA, that coats the viral lipid membrane is composed of a head domain and a stalk domain. Classically, 5 antigenic sites were identified in the head domain of the laboratory-adapted H1N1 strain, A/Puerto Rico/8/1934 (PR8) (8). These antigenic sites, defined as Sa, Sb, Ca1, Ca2, and Cb (Figure 1A), were characterized using virus escape mutants and a panel of monoclonal antibodies (9). Sa and Sb are located on the distal tip of each HA monomer, while Ca1, Ca2, and Cb are located proximally, near the stalk domain. Virus-host attachment occurs at the sialic acid receptor binding domain (RBD) located between Sb, Ca2, and Sa (10).

Monoclonal antibodies showing hemagglutination inhibition (HI) activities to each of the 5 antigenic sites have been characterized (11, 12). Serum HI titers are a major correlate for protection against influenza-related illness in adults and children (13, 14). Significant efforts have been made to define a hierarchy of HI activities for the antigenic sites of the HA head to guide vaccine design. Angeletti et al. showed that antisera from BALB/c mice infected with PR8 had a greater number of antibodies targeting Sb, followed by Sa, Cb, Ca2, and then Ca1 (12). Using antisera from ferrets infected with pre-2009 H1N1 strains, Koel et al. showed that the greatest reductions in HI titers were due to amino acid mutations proximal to the RBD (15). The HI hierarchy for the H1 vaccine strain, A/Michigan/45/2015, remains undefined. Additionally, HI hierarchies comparing all 5 antigenic sites of pH1N1 have never been established for the immune responses of humans. The present study used a reverse genetics system to create a panel of mutant viruses encoding mutant HAs that lack 1 of the 5 HI active antigenic sites. When antisera to A/Michigan/45/2015 were tested against this panel of mutant viruses, relative reductions in HI titers defined the HI dominances of specific antigenic sites.

▶ Related Commentary: https://doi.org/10.1172/JCI124151

**Authorship note:** MAB and WS contributed equally to this work.
**Conflict of interest:** The authors have declared that no conflict of interest exists.

**Submitted:** June 25, 2018; **Accepted:** August 21, 2018.
**Reference information:** *J Clin Invest*. https://doi.org/10.1172/JCI122895.

## Results and Discussion

*Creation of a mutant virus panel for A/Michigan/45/2015*. Using a reverse genetics system (16), a panel of 5 mutant viruses (H1-ΔSa, H1-ΔSb, H1-ΔCa1, H1-ΔCa2, H1-ΔCb) was created in which classically defined H1 antigenic sites (Sa, Sb, Ca1, Ca2, and Cb, respectively) were partially substituted with heterologous antigenic sites from either H5 or H13 HAs (Figure 1B). Mutant viruses were designed with an HA encoded by A/Michigan/45/2015 and the 7 remaining segments encoded by PR8. Previous observations sug-

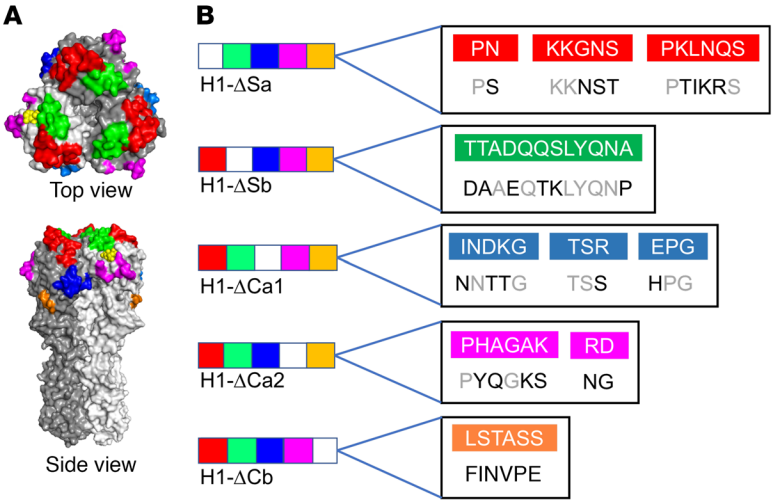


**Figure 1. Head domain epitopes of pandemic-like H1 HA and amino acid sequences of mutant epitope substitutions.** (**A**) Crystal structure of pandemic H1 HA trimer (PDB:3UBE) (10) (top view and side view, 1 monomer in white and 2 monomers in gray) with classically defined antigenic sites colored as follows: Sa in red, Sb in green, Ca1 in blue, Ca2 in magenta, and Cb in orange. Modeling performed with PyMOL (The PyMOL Molecular Graphics System, Version 2.0.1, Schrödinger, LLC). A sialic acid molecule (yellow) is present in the receptor binding pocket of the white HA monomer. (**B**) Amino acid sequences of the antigenic sites of pandemic-like H1 strain A/Michigan/45/2015 are highlighted as follows: Sa in red, Sb in green, Ca1 in blue, Ca2 in magenta, and Cb in orange. Amino acid sequences of heterologous epitopes for the mutant virus panel are listed below the respective pandemic H1 sites. Amino acids in black represent substituted residues. Amino acids in gray are unchanged.

gested that antigenically drifted influenza virus strains generally have 4 or more amino acid substitutions in 2 or more antigenic sites (17). To ensure the loss of antigenicity for an individual antigenic site, each mutant virus in our panel contained 5 or more amino acid substitutions within 1 antigenic site. Additionally, several amino acid substitutions that were included in our panel were consistent with previously described escape mutations (18). While our study focused on the classically defined epitopes of pandemic H1 hemagglutinin, several nonclassical epitopes have been described as being HI sensitive (11, 19, 20). To measure the HI activities of these nonclassical epitopes, 2 additional mutant viruses were constructed: a mosaic H5/1 virus (mH5/1), in which all 5 classically defined H1 epitopes were replaced with H5-like epitopes, leaving the nonclassical epitopes intact; and a chimeric H5/1 (cH5/1), in which the entire H1 head domain was replaced with an H5 head domain. All mutant viruses were plaque purified and sequenced. All viruses showed high hemagglutination activities toward chicken red blood cells, which allowed us to use chicken red blood cells for subsequent HI assays. Egg-adaptive mutations were rare. In summary, a robust panel of mutant viruses lacking antigenic epitopes in the head domain was rescued.

*HI profiles of animal antisera*. Naive mice, guinea pigs, and ferrets were intranasally infected with $10^5$ PFU of A/Michigan/45/2015 virus (H1N1). Sera were collected 4 weeks after infection (except for 2 of the 5 ferret antisera, which were collected at 3 weeks after infection). Animal antisera showed high HI titers (>1:160) against the WT H1 virus. Ferret antisera had the highest HI titers against WT H1 virus, followed by mouse antisera then guinea pig antisera. HI assays with the panel of mutant viruses (see Figure 1B) revealed the greatest reductions in HI titers to mutant viruses containing substitutions surrounding the RBD. As discussed in a recent paper by Altman et al., immunodominance hierarchy may be different for genetically different mouse strains (21). BALB/c mice were used for this study. Mouse antisera had significant reductions in HI titers against H1-ΔSb and H1-ΔCa2. Minimal reductions were observed against H1-ΔSa, H1-ΔCb,

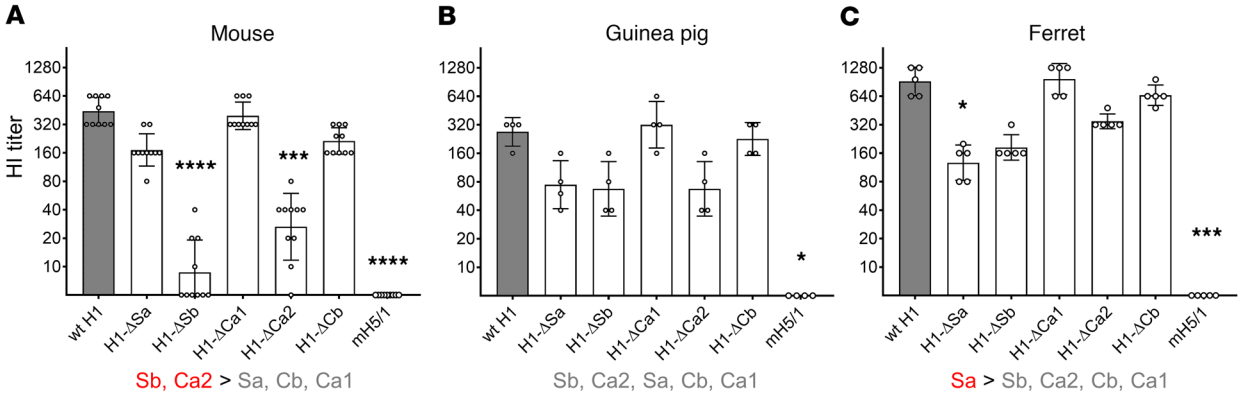


**Figure 2. HI profiles of antisera from mice, guinea pigs, and ferrets.** Hemagglutination inhibition titers of mouse ($n$ = 10) (**A**), guinea pig ($n$ = 4) (**B**), and ferret ($n$ = 5) (**C**) antisera were measured against a panel of mutant viruses (see Figure 1B). Naive animals were intranasally infected with $1 \times 10^5$ PFU of a pandemic-like H1N1 virus, A/Michigan/45/2015, and antisera were harvested at 4 weeks after infection (except for 2 ferret antisera, which were harvested at 3 weeks after infection). The HI profiles for each species are listed; statistically significant reductions are in red and minimal reductions are in gray. Experiments were performed in technical duplicates. Circles represent averaged HI titers of an individual animal's serum. Bars represent the geometric mean ± geometric SD. Statistical significance was determined between the mutant virus to the WT H1 virus using Dunn's corrected Kruskal-Wallis 1-way ANOVA of the mean HI titers (*$P \le 0.05$, ***$P \le 0.001$, ****$P \le 0.0001$).

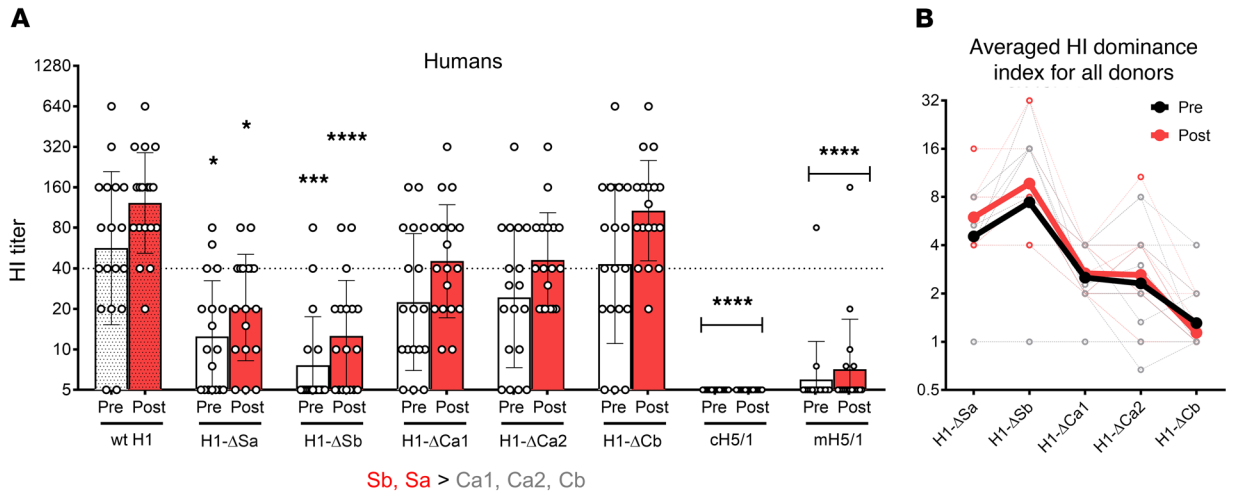


**Figure 3. HI profiles for adult humans before and after 2017–2018 seasonal vaccination.** (**A**) HI activities of plasma samples ($n$ = 36) collected from 18 adult donors before and after seasonal vaccination (white and red, respectively), measured against a panel of mutant viruses (see Figure 1). The human HI profile is listed; statistically significant reductions are in red and minimal reductions are in gray. Experiments were performed in technical duplicates. Circles represent averaged HI titers of an individual donor's serum. Bars represent the geometric mean ± geometric SD. Statistical significance was determined between the mutant virus to the respective WT H1 virus data set (before or after vaccination) using Dunn's corrected Kruskal-Wallis 1-way ANOVA of the mean HI titers (*$P \le 0.05$, ***$P \le 0.001$, ****$P \le 0.0001$). (**B**) An HI dominance index was calculated for individual samples against each mutant virus (from A). The HI dominance index represents a fold reduction of HI titer in a mutant virus versus its respective WT H1 virus. Single individuals are represented by dotted lines. Averaged HI dominance indices for before (Pre, black) and after (Post, red) vaccination are plotted in solid lines.

and H1-ΔCa1 (Figure 2A). Guinea pig antisera showed no significant reductions for any specific site, but minimal reductions in HI titers trended toward H1-ΔSb, H1-ΔCa2, and H1-ΔSa viruses (Figure 2B). Ferret antisera had a significant reduction in the HI titer against H1-ΔSa (Figure 2C). Although a statistically significant reduction in the Sa response was observed in ferrets and not guinea pigs, the biological relevance of this difference remains unclear due to the limited sample sizes. Using a panel of mutant viruses, HI hierarchies have been established for the antibody responses of mice, guinea pigs, and ferrets. These results support previous animal studies demonstrating the importance of the HI active antigenic sites surrounding the RBD (12, 15).

*Seasonal vaccination maintains the HI profile of humans.* Human plasma samples were collected from 18 adult volunteers prior to vaccination with 2017–2018 seasonal vaccines and more than 4 weeks after vaccination. Study participants varied in age, sex, sample collection times, and specific types of vaccination (Supplemental Table 1; supplemental material available online with this article; https://doi.org/10.1172/JCI122895DS1). Human plasma samples were tested for HI activity against the WT H1 virus and against the panel of mutant viruses (see Figure 1B). There was a broad range of HI titers observed against WT H1 virus (Figure 3A). Generally, HI titers against all viruses increased upon seasonal vaccination. Geometric mean analysis of the prevaccination antisera showed significant reductions in HI titers against H1-ΔSb and H1-ΔSa. H1-ΔCa1 and H1-ΔCa2 showed minimal but insignificant reductions. H1-ΔCb showed similar HI titers to WT H1 virus. The averaged HI profile of the human cohort was preserved in the postvaccination antisera. These results confirm that the HI activities of human plasma mostly depend on the antigenic sites surrounding the RBD.

An HI dominance index was created to help analyze the data sets (Figure 3B). The HI dominance index equals the fold reduction in HI titer of a specific mutant virus compared with the respective WT H1 virus. By plotting the HI dominance indices of all 5 mutant viruses, subtle shifts in averaged HI dominance due to seasonal vaccination were revealed. A closer analysis of the HI profile of each individual donor showed wide variations in HI profiles for both pre- and postvaccination antisera (Supplemental Figure 1). Unfortunately, due to the relatively small number of study participants, our analysis was not powered to detect any potential correlations between HI profiles and patient demographics.

HI titers were not detected in donor samples using the cH5/1 virus, which displays a head domain to which humans are typically naive. Although evidence suggests that immunization to the 2009 pandemic vaccine may elicit an antibody response that is broadly cross-reactive with the potential to bind H1, H5, and H3 hemagglutinins, these antibodies target the HA stem and are not active in HI assays (22). Interestingly, HI activity was detected with the mH5/1 virus, a virus lacking all 5 classically defined antigenic sites. Two of 18 donors had HI titers against mH5/1 in prevaccination samples, and 5 of 18 donors developed HI titers after vaccination. The detection of these HI titers suggests that naturally occurring antibody responses against nonclassical HA-head epitopes are uncommon but can be boosted by immunization. It is possible that the mH5/1 virus may contain incompletely substituted epitopes that are targeted upon vaccination. However, this is unlikely given that the antisera of all animals infected with WT H1 did not show any HI titers to the mH5/1 virus (Figure 2). Another explanation for the HI activities against mH5/1 could be the presence of antibodies that target the receptor binding pocket directly using a long CDR3 region. Such monoclonal antibodies have been isolated from humans and typically exhibit binding that is independent of mutations in the major antigenic sites (20, 23–25).

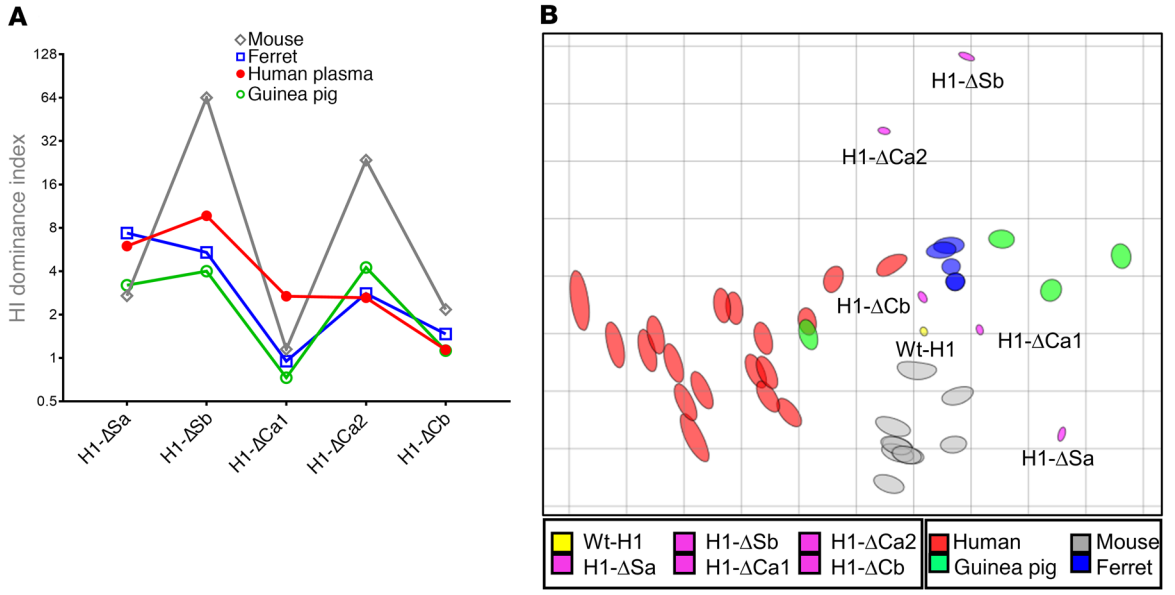


**Figure 4. Species-specific HI profiles.** (**A**) HI dominance indices of postvaccination human plasma (taken for comparison from Figure 3B) and antisera of infected mice, ferrets, and guinea pigs were plotted. (**B**) Absolute HI titers of postvaccination human plasma and antisera of infected mice, ferrets, and guinea pigs were mapped by antigenic cartography (27). Plots were created from a reanalysis of the data sets shown in Figure 2A and Figure 3.

HI profiling offers a new method to measure immune responses in individuals whose HI titers do not change against WT H1 virus after vaccination. This is important since antigenic site immunodominance could change even in the absence of an increase in total HI activity. Seven of the 18 donors (39%) did not change their HI titers against WT H1 virus (donors A, F, G, I, L, M, and Q of Supplemental Figure 2). Of these 7 donors, only 3 donors (G, I, Q) showed no changes in their HI profiles before and after vaccination. Overall, 4 donors (C, E, K, R) became Sb dominant. Six donors (B, D, H, L, N, O) developed Sa and Sb codominance upon vaccination. Three donors (A, F, M) maintained their Sb dominance but had reductions in the intensity of Sb dominance. It will be interesting to see if isolated changes in HI profiles would be sufficient to confer protection toward drifted strains.

*Comparison of species-specific HI profiles*. This study provides a comparison of HI profiles among different species. Despite similar tendencies to target the RBD, animals and humans have distinct HI profiles. These differences can be seen when plotting the averaged HI dominance indices of all of the species together (Figure 4A). Ferrets and humans have higher Sa HI dominance indices than mice and guinea pigs. Mice have particularly high HI dominance indices for Sb and Ca2. The Ca1 HI dominance index of humans is higher than the Ca1 HI dominance indices of all 3 tested animal species.

Differences in HI profiles can also be visualized with antigenic cartography (Figure 4B). Mapping the HI titers of different species is possible because the HI assays were all performed with chicken red blood cells and the antisera of animals and humans were all exposed to WT A/Michigan/45/2015 virus. Furthermore, the antiserum from an individual's plasma and serum samples have a high degree of agreement for HI titers against H1 influenza (26). Clear divisions appear among human, ferret, and mouse antisera. Ferret antisera are tightly grouped, whereas mouse, guinea pig, and human antisera are broadly distributed and less superimposed. A single guinea pig antiserum interestingly overlaps with human antisera. This may be an outlier due to the limited number of animals studied during this investigation, or it may be a consequence of the genetic variations of outbred guinea pigs. The differences among laboratory animals may be driven by species-specific immune responses as well as species-specific viral pathogenesis. When comparing the human profiles to the small mammal profiles these factors should be considered, in addition to differences in exposure route (e.g., immunization versus infection) and exposure history. These observations are intriguing and warrant future species-to-species direct comparisons. Longitudinal monitoring with larger cohorts of human donors will be required to assess whether HI titers against specific antigenic sites may correlate strongly with protection against influenza-related illness.

## Methods

For additional information, see Supplemental Methods.

*Study approval*. The Icahn School of Medicine at Mount Sinai IRB approved the human studies. Informed consent was received from participants prior to inclusion in the study. Animal experiments were performed in accordance with protocols approved by the IACUC at the Icahn School of Medicine at Mount Sinai.

*Statistics*. Statistical data were generated with the GraphPad Prism program version 7.02. Statistical significance between groups was determined by performing 1-way ANOVA with Dunn's corrected Kruskal-Wallis test, where $P \leq 0.05$ was considered significant.

## Author contributions

STHL, WS, FB, RN, FK, VS, RAA, NMB, and PP designed the study. VS (Personalized Virology Initiative) provided human samples. STHL, MAB, AWF, WCL, RAA, and NMB conducted experiments and acquired data. STHL, RN, FK, WS, FB, AWF, and MAB analyzed the data. STHL and PP drafted the manuscript, with final editing from all authors.

## Acknowledgments

This work was supported by NIH, National Institute of Allergy and Infectious Disease (NIAID) grants 5T32AI007647-18, U19 AI109946, and P01AI097092, and the NIH/NIAID Centers of Excellence for Influenza Virus Research and Surveillance (CEIRS) contract HHSN272201400008C. We thank Maria Bermudez-Gonzalez, Mark Bailey, Jim Duehr, Dionne Argyle, Allen Zheng, and Chen Wang for their help. We also acknowledge generous philanthropic support for the Personalized Virology Initiative.

Address correspondence to: Peter Palese, Annenberg Building, 16th Floor, 1468 Madison Avenue, New York, New York 10029, USA. Phone: 212.241.7318; Email: peter.palese@mssm.edu.

1. Budd AP, et al. Update: influenza activity - United States, October 1, 2017-February 3, 2018. *MMWR Morb Mortal Wkly Rep*. 2018;67(6):169–179.
2. Nichol KL, et al. The effectiveness of vaccination against influenza in healthy, working adults. *N Engl J Med*. 1995;333(14):889–893.
3. Flannery B, et al. Interim estimates of 2017-18 seasonal influenza vaccine effectiveness - United States, February 2018. *MMWR Morb Mortal Wkly Rep*. 2018;67(6):180–185.
4. Erbelding EJ, et al. A universal influenza vaccine: the strategic plan for the National Institute of Allergy and Infectious Diseases. *J Infect Dis*. 2018;218(3):347–354.
5. Paules CI, Sullivan SG, Subbarao K, Fauci AS. Chasing seasonal influenza - the need for a universal influenza vaccine. *N Engl J Med*. 2018;378(1):7–9.
6. Grohskopf LA, et al. Prevention and control of seasonal influenza with vaccines: recommendations of the Advisory Committee on Immunization Practices - United States, 2017-18 influenza season. *MMWR Recomm Rep*. 2017;66(2):1–20.
7. Knipe DM, Howley PM. *Fields Virology*. 6th ed. Philadelphia, PA: Wolters Kluwer/Lippincott Williams & Wilkins Health; 2013.
8. Caton AJ, Brownlee GG, Yewdell JW, Gerhard W. The antigenic structure of the influenza virus A/PR/8/34 hemagglutinin (H1 subtype). *Cell*. 1982;31(2 Pt 1):417–427.
9. Gerhard W, Yewdell J, Frankel ME, Webster R. Antigenic structure of influenza virus haemagglutinin defined by hybridoma antibodies. *Nature*. 1981;290(5808):713–717.
10. Xu R, McBride R, Nycholat CM, Paulson JC, Wilson IA. Structural characterization of the hemagglutinin receptor specificity from the 2009 H1N1 influenza pandemic. *J Virol*. 2012;86(2):982–990.
11. Matsuzaki Y, et al. Epitope mapping of the hemagglutinin molecule of A/(H1N1)pdm09 influenza virus by using monoclonal antibody escape mutants. *J Virol*. 2014;88(21):12364–12373.
12. Angeletti D, et al. Defining B cell immunodominance to viruses. *Nat Immunol*. 2017;18(4):456–463.
13. Ohmit SE, Petrie JG, Cross RT, Johnson E, Monto AS. Influenza hemagglutination-inhibition antibody titer as a correlate of vaccine-induced protection. *J Infect Dis*. 2011;204(12):1879–1885.
14. Coudeville L, Bailleux F, Riche B, Megas F, Andre P, Ecochard R. Relationship between haemagglutination-inhibiting antibody titres and clinical protection against influenza: development and application of a bayesian random-effects model. *BMC Med Res Methodol*. 2010;10:18.
15. Koel BF, et al. Substitutions near the receptor binding site determine major antigenic change during influenza virus evolution. *Science*. 2013;342(6161):976–979.
16. Chen CJ, Ermler ME, Tan GS, Krammer F, Palese P, Hai R. Influenza A viruses expressing intra- or intergroup chimeric hemagglutinins. *J Virol*. 2016;90(7):3789–3793.
17. Wilson IA, Cox NJ. Structural basis of immune recognition of influenza virus hemagglutinin. *Annu Rev Immunol*. 1990;8:737–771.
18. Retamal M, Abed Y, Corbeil J, Boivin G. Epitope mapping of the 2009 pandemic and the A/Brisbane/59/2007 seasonal (H1N1) influenza virus haemagglutinins using mAbs and escape mutants. *J Gen Virol*. 2014;95(Pt 11):2377–2389.
19. Zhao R, et al. Identification of a highly conserved H1 subtype-specific epitope with diagnostic potential in the hemagglutinin protein of influenza A virus. *PLoS One*. 2011;6(8):e23374.
20. Krause JC, Tsibane T, Tumpey TM, Huffman CJ, Basler CF, Crowe JE. A broadly neutralizing human monoclonal antibody that recognizes a conserved, novel epitope on the globular head of the influenza H1N1 virus hemagglutinin. *J Virol*. 2011;85(20):10905–10908.
21. Altman MO, Angeletti D, Yewdell JW. Antibody immunodominance: the key to understanding influenza virus antigenic drift. *Viral Immunol*. 2018;31(2):142–149.
22. Li GM, et al. Pandemic H1N1 influenza vaccine induces a recall response in humans that favors broadly cross-reactive memory B cells. *Proc Natl Acad Sci U S A*. 2012;109(23):9047–9052.
23. Ekiert DC, et al. Cross-neutralization of influenza A viruses mediated by a single antibody loop. *Nature*. 2012;489(7417):526–532.
24. Tsibane T, et al. Influenza human monoclonal antibody 1F1 interacts with three major antigenic sites and residues mediating human receptor specificity in H1N1 viruses. *PLoS Pathog*. 2012;8(12):e1003067.
25. Whittle JR, et al. Broadly neutralizing human antibody that recognizes the receptor-binding pocket of influenza virus hemagglutinin. *Proc Natl Acad Sci U S A*. 2011;108(34):14216–14221.
26. Defang GN, et al. Comparative analysis of hemagglutination inhibition titers generated using temporally matched serum and plasma samples. *PLoS One*. 2012;7(12):e48229.
27. Smith DJ, et al. Mapping the antigenic and genetic evolution of influenza virus. *Science*. 2004;305(5682):371–376.